Pharmaceutical Research, Vol. 27, No. 1, January 2010 (© 2009)
DOI: 10.1007/s11095-009-9998-8

Research Paper

Porphyrin and Galactosyl Conjugated Micelles for Targeting Photodynamic Therapy

De-Qun Wu,[1] Ze-Yong Li,[1] Cao Li,[1] Jian-Jun Fan,[1] Bo Lu,[1] Cong Chang,[1] Si-Xue Cheng,[1] Xian-Zheng Zhang,[1,2] and Ren-Xi Zhuo[1]

Received June 10, 2009; accepted October 15, 2009; published online November 4, 2009

Purpose. To study the targeting and photodynamic therapy efficiency of porphyrin and galactosyl conjugated micelles based on amphiphilic copolymer galactosyl and mono-aminoporphyrin (APP) incoporated poly(2-aminoethyl methacrylate)-polycaprolactone (Gal-APP-PAEMA-PCL).
Methods. Poly(2-aminoethyl methacrylate)-polycaprolactone (PAEMA-PCL) was synthesized by the combination of ring opening polymerization and reversible addition-fragmentation chain transfer (RAFT) polymerization, and then Gal-APP-PAEMA-PCL was obtained after conjugation of lactobionic acid and 5-(4-aminophenyl)-10,15,20-triphenylporphyrin (APP) to PAEMA-PCL. The chemical structures of the copolymers were characterized, and their biological properties were evaluated in human laryngeal carcinoma (HEp2) and human hepatocellular liver carcinoma (HepG2) cells.
Results. Both APP-PAEMA-PCL and Gal-APP-PAEMA-PCL did not exhibit dark cytotoxicity to HEp2 cells and HepG2 cells. However, Gal-APP-PAEMA-PCL was taken up selectively by HepG2 cells and had the higher phototoxicity effect. Both polymers preferentially localized within cellular vesicles that correlated to the lysosomes.
Conclusions. The results indicated that porphyrin and galactosyl conjugated polymer micelles exhibited higher targeting and photodynamic therapy efficacy in HepG2 cells than in HEp2 cells.

KEY WORDS: drug delivery; galactosyl micelle; phototoxicity; porphyrin.

INTRODUCTION

Photodynamic therapy (PDT) is a method using light to irradiate photosensitizers (PSs) to produce intracellular reactive oxygen species (ROS) that kill cells (1,2). Due to the preferential distribution and retention of PSs in neoplastic tissues and the location of phototoxic effect, PDT is an attractive minimally invasive treatment protocol for cancers and several neovascular diseases (3). In addition, compared with immunosuppression of common cancer therapies, such as radiation therapy and chemotherapy, PDT has favorable pharmaceutical properties, since it can activate the immune response (4).

In PDT, the PSs absorb light with appropriate wavelength at the site of the photodynamic reaction to produce ROS to induce cellular toxicity. One of the most extensively studied PSs so far is porphyrin, which contains porphyrinic structure with four pyrrole rings connected by methine bridges in a cyclic configuration. Because of the π-π interactions and hydrophobic characteristics, conventional PSs can easily form aggregates, which cause self-quenching effect of the excited state in the aqueous medium. To obtain high quantum yields and effective energy absorption, PSs were segregated into focal core of dendrimers in previous literature (5). Chemical modifications of porphyrin derivatives were also carried out to improve their performance and post-treatment skin sensitivity (6,7). To selectively deliver the porphyrin sensitizers to tumor tissues, several strategies have been developed, including the conjugations of porphyrin moiety with oligonucleotides (8), carrier proteins (9), epidermal growth factors (10), monoclonal antibodies (11), carbohydrates (12), and hydrophilic polymers, such as N-(2-hydroxypropyl)methacrylamide (HPMA) (13) and polylysine (14). In addition, cationic porphyrins have received a great deal of interest due to their DNA binding properties. It is known that some porphyrin derivatives can intercalate into DNA, so that they could be retained longer in carcinoma cells than in normal cells (15), resulting in enhanced light-induced mitochondrial damage and cell killing (16).

The micellar systems self-assembled from amphiphilic copolymers have been extensively investigated due to their obvious advantages, such as prolonged circulation in the blood, improved stability, and enhanced accumulation in tumor tissue (17,18). In order to endow the specific recognition of the micelles by a specific site, targeting ligands, such as folic acid, antibodies, RGD, etc., have been introduced to the micelles or nanoparticles (19). It was reported that

Electronic supplementary material The online version of this article (doi:10.1007/s11095-009-9998-8) contains supplementary material, which is available to authorized users.

[1] Key Laboratory of Biomedical Polymers of Ministry of Education, Department of Chemistry, Wuhan University, Wuhan 430072, China.
[2] To whom correspondence should be addressed. (e-mail: xz-zhang@whu.edu.cn)

asialoglycoprotein (ASGP) receptors were expressed plentifully on the surface of hepatoma cells and mammalian hepatocytes, and targeting could be accomplished through introduction of galactose residues, which can bind specifically to the ASGP receptors on the cells (20–23).

Herein, we synthesized galactosyl and porphyrin incorporated amphiphilic copolymer Gal-APP-PAEMA-PCL. Owing to the galactosyl moiety conjugated to the polymer, the self-assembled Gal-APP-PAEMA-PCL micelles can be selectively bound to ASGP receptors on the surfaces of HepG2 cells. Since the porphyrin moiety was connected to the hydrophilic part of the polymer, the aggregation of the porphyrin in aqueous media could be avoided, and thus the quantum yield and effective energy absorption could be improved, which resulted in the improved photodynamic efficacy. The cell internalization of Gal-APP-PAEMA-PCL micelles was schematically demonstrated in Scheme 1.

MATERIALS AND METHODS

Materials

ε-Caprolactone (CL) from Acros was dried over CaH_2 for 48 h, distilled under reduced pressure, and stored under inert atmosphere. Lactobionic acid (LBA), diglycolic anhydride (DA), and 2-aminoethyl methacrylate hydrochloride (AEMA·HCl) were purchased from Acros. Tetrahydrofuran (THF) and dimethyl sulfoxide (DMSO) were obtained from Shanghai Chemical Reagent Co., China, and used after distillation under reduced pressure. Ethyl acetate, dichloromethane (DCM), stannous octoate ($Sn(Oct)_2$), heptane, 4-nitrobenzaldehy, pyrrole, 1-nitrobenzene, fuming nitric acid, triethylamine (TEA), 2,2′-azobis(isobutyronitrile) (AIBN), 1-bromobenzene, magnesium, 1-bromoacetic acid, carbon bisulfide, 2-hydroxyethyl methacrylate N,N′-dicyclohexylcarbodiimide (DCC) and 4-(*N,N*-dimethylamino)-pyridine (DMAP) were obtained from Shanghai Chemical Reagent Co., China. Molecular Probes (MitoTracker Green, LysoSensor Green, BODIPY FLC5-Ceramide, and DiOC6), Dulbecco's modified Eagle's medium (DMEM), and HEPES were purchased from GIBCO invitrogen corporation.

^{1}H Nuclear Magnetic Resonance

^{1}H nuclear magnetic resonance (^{1}H NMR) spectra were recorded on a Mercury VX-300 spectrometer at 300 MHz (Varian, USA) by using D_2O or DMSO-d_6 as a solvent and TMS as an internal standard.

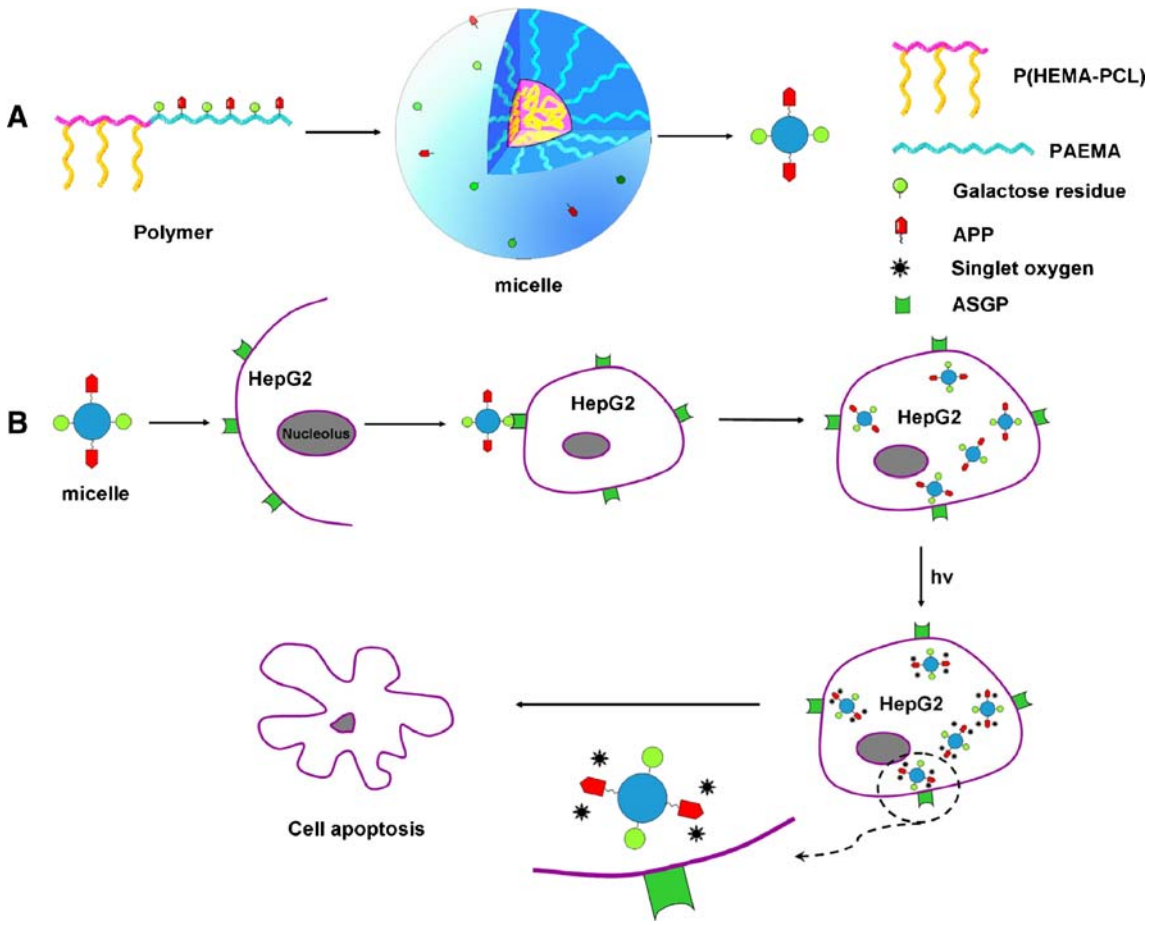

Scheme 1. **A** Schematic representation of the core-shell micelle self-assembled from Gal-APP-PAEMA-PCL, and **B** the liver-targeting mechanism and phototoxicity of Gal-APP-PAEMA-PCL.

Fourier Transform Infrared Spectroscopy

Fourier transform infrared spectroscopy (FT-IR) spectra were recorded on an AVATAR 360 spectrometer. Samples were pressed into potassium bromide (KBr) pellets.

Gel Permeation Chromatography

The molecular weight of the polymers was obtained by a gel permeation chromatographic system equipped with a Waters 2690D separations module and a Waters 2410 refractive index detector. Gel permeation chromatography (GPC) were conducted using a Waters-2690D equipped with Styragel columns for HEMA-PCL with a concentration of 8 mg/mL using THF as eluent, while Ultrahydrogel GPC columns were used for PAEMA with a concentration of 8 mg/mL using a buffer solution (pH 3.3) containing 0.30 M NaH_2PO_4 and 1.0 M acetic acid at a flow rate of 0.3 mL/min. Waters millennium module software was used to calculate the molecular weight on the basis of universal calibration curves generated by polystyrene standards for HEMA-PCL and polyethylene glycol standards for PAEMA.

Synthesis of Reversible Addition-Fragmentation Chain-Transfer Agent 2-(Phenylcarbonothioylthio) Acetic Acid

1-Bromobenzene (25.0 g, 160 mmol) was added to a round-bottomed flask containing anhydrous tetrahydrofuran (250 mL), magnesium turnings (4.0 g, 167 mmol), and iodine. The reaction mixture was heated to 80°C and allowed to reflux for 2 h until no magnesium could be observed. The reaction mixture was then cooled to 0°C, and carbon disulfide (40.1 g, 528 mmol) was introduced dropwise. After a color change from clear to deep orange was observed, the reaction system was allowed to reach room temperature. To this reaction system, 1-bromoacetic acid (22.0 g, 160 mmol) in anhydrous tetrahydrofuran was added by syringe. The temperature was raised to 100°C and maintained for 24 h, and the crude product was concentrated by removal of solvent in vacuum and then dissolved in ethyl acetate. The product was isolated by extracting into the aqueous layer using sodium hydroxide solution (1 M, 500 mL) and then returned to a fresh layer of ethyl acetate using HCl solution (1 M, 500 mL). The product 2-(phenylcarbonothioylthio) acetic acid (CTA) (purity>99%) was isolated as orange crystals by recrystallization in a mixture of ethyl acetate and hexane (v/v=1:50) with a yield of 50%. ^{1}H NMR (DMSO-d_6, 300 MHz): δ (ppm from TMS) 5.36 (2H, C-H), 7.58 (2H, Ar-H), 7.78 (1H, Ar-H), 8.02 (2H, Ar-H), 13.02 (COO-*H*) (Fig. S1 in Supplementary Material).

Synthesis of 5-(4-Aminophenyl)-10,15,20-Triphenylporphyrin

Tetraphenylporphyrin (H_2TPP) and 5-(4-nitrophenyl)-10,15,20-triphenylporphyrin (NPP) were synthesized according to the literature (24,25). NPP (2.0 g, 3.03 mmol) was dissolved in 64 mL of concentrated hydrochloric acid under nitrogen atmosphere. Tin(II) chloride dihydrate (2.1 g, 9.2 mmol) was added to the solution, and the reaction was carried out at 65°C for 1 h. The resulted solution was cooled. Then 300 mL of cold water was added, and pH was adjusted to 8 with concentrated sodium hydroxide. The aqueous phase was extracted with 5× 300 mL of chloroform, which were dried over magnesium sulfate. The organic phase was concentrated on a rotary evaporator to 100 mL, and the solution was chromatographed through silica column with methylene chloride as an eluent to obtain 5-(4-aminophenyl)-10,15,20-triphenylporphyrin (APP) (purity>99%) with a yield of 30%. ^{1}H NMR (DMSO-d_6, 300 MHz) δ 8.92 ppm (2 H, β-pyrrole) 8.83 ppm (2 H, β-pyrrole), 8.81 ppm (2 H, β-pyrrole) 8.20 ppm (6 H, ortho triphenyl), 8.00 ppm (2 H, 4-aminophenyl), 7.74 ppm (9 H, meta/para triphenyl), 7.06 (2 H, 4-aminophenyl), 5.62 (2 H, amino), −2.88 ppm (2 H pyrrole NH); ESI-MS m/z 630.5 ($M+H^+$), calculated for $C_{44}H_{31}N_5$ 630.3 (Fig. S2, S3 in Supplementary Material).

Synthesis of 5-(4-Aminophenyl)-10,15,20-Triphenylporphyrin-Diglycolic Anhydride

To a solution of APP (0.50 g, 0.795 mmol) in DMF (4 mL), diglycolic anhydride (DA) (0.14 g, 1.19 mmol) was added, and the mixture was stirred at room temperature overnight. The reaction system was diluted with 15 mL of $CHCl_3$, followed by hexane until precipitation occurred. The precipitate was filtered and washed with water to remove residual anhydride and then dried under vacuum to obtain 5-(4-aminophenyl)-10,15,20-triphenylporphyrin-diglycolic anhydride (APP-DA) (purity>95%) with a yield of 98%. ^{1}H NMR (DMSO-*d*6, 300 MHz): δ 10.42 (1H, COO-H), 8.85–8.91 (8H), 8.18–8.32 (10 H), 7.84–7.89 (9H), 4.30–4.34 (4H), -2.92 (2H). ESI-MS m/z 746.4 ($M+H^+$), calculated for $C_{48}H_{35}N_5O_4$ 746.3 (Fig. S2, S4 in Supplementary Material).

Synthesis of 2-Hydroxyethyl Methacrylate-Poly(ε-Caprolactone)

2-Hydroxyethyl methacrylate-poly(ε-caprolactone) (HEMA-PCL) was synthesized according to our previous report (26). Briefly, ε-caprolactone (17.10 g, 0.15 mol), HEMA (3.90 g, 0.03 mol), and catalyst $SnOct_2$ (0.12 g, 0.1 mol % with respect to HEMA) were added into a glass ampoule with a magnetic bar. Then, 2,6-di-*tert*-butyl-4-methylphe-nol (0.067 g) was added, and the ampoule was sealed under vacuum. The ampoule was immersed in an oil bath at 120°C for 3 h. The product was collected by dissolving the cooled reaction mixture in methylene dichloride and precipitating at least twice in 10-fold chilled methanol. After vacuum drying for 48 h, HEMA-PCL was obtained in 72% yield.

Synthesis of Poly(2-Aminoethyl Methacrylate)

Reversible addition-fragmentation chain-transfer (RAFT) polymerization of AEMA was carried out at 70°C, using AIBN as the radical initiator and CTA as the RAFT chain transfer agent. A typical protocol was performed as follows. In a 25 mL flask, AEMA·HCl (4.14 g, 25 mmol) was dissolved in anhydrous DMSO (10 mL), and then AIBN (8.75 mg, 0.05 mmol) and CTA (53.0 mg, 0.25 mmol) were added. After degassing via three freeze-thaw cycles, the flask was placed in an oil bath at 70°C for 24 h with vigorous stirring. The resultant product was purified by dialysis against

distilled water to remove unreacted AEMA monomer and DMSO and then freeze-dried to obtain poly(2-aminoethyl methacrylate)(PAEMA) (yield 78%).

Synthesis of Poly(2-Aminoethyl Methacrylate)-Poly(ε-Caprolactone)

PAEMA (3.0 g, 18 mmol) was dissolved in anhydrous DMSO (10 mL) and then mixed with HEMA-PCL (1.50 g, 7.5 mmol) and AIBN (2.63 mg, 0.015 mmol) in a 50 mL flask, which was subsequently degassed by three freeze-thaw cycles. The polymerization was carried out at 70°C in an oil bath with continuous stirring for 24 h. The product was purified by precipitating in DCM and then dissolving in DMSO, dialysis against water to remove DMSO. After freeze-drying, poly(2-aminoethyl methacrylate)-poly(ε-caprolactone) (PAEMA-PCL) was obtained (yield 75%).

Synthesis of Galactosyl and Mono-Aminoporphyrin Incoporated Poly(2-Aminoethyl Methacrylate)-Polycaprolactone

Lactobionic acid (10.0 g) and a small amount of trifluoroacetic acid were dissolved in anhydrous methanol (100 mL), and the reaction was carried out at 50°C under vacuum for 3 h. The above process was repeated at least thrice until lactobionic acid was fully converted to the lactobionolactone. Then PAEMA-PCL (1.0 g) was dissolved in anhydrous DMSO (15 mL), and TEA was added to adjust the solution pH value to 8. Lactobionolactone (0.25 g) was added to the above solution, and the reaction was carried out for 8 h. The product was purified by dialysis against distilled water to remove the unreacted LBA and DMSO, and then poly(2-aminoethyl methacrylate)-polycaprolactone (Gal-PAEMA-PCL) was collected after freeze-drying (yield 72%).

APP-DA (0.14 g, 0.184 mmol) was dissolved in DMSO (10 mL), and then DCC (45.5 mg, 0.22 mmol) and NHS (27.7 mg, 0.226 mmol) were added. The mixture was stirred at room temperature under nitrogen atmosphere for 1 day. Precipitated dicyclohexylurea (DCU) was removed by filtration. Then, the obtained solution was mixed with Gal-PAEMA-PCL to carry out the reaction at room temperature under nitrogen atmosphere for 1 day. The product was purified by dialysis against DMSO for 3 days, then dialysis against distilled water for 3 days, and finally freeze-drying to obtain Gal-APP-PAEMA-PCL (yield 68%).

Determination of Critical Micelle Concentration

Fluorescence spectra were recorded on a LS55 luminescence spectrometer (Perkin-Elmer), and the method was reported elsewhere (27,28). In brief, pyrene was used as a hydrophobic fluorescent probe. Aliquots of pyrene solutions (6×10^{-6} M in acetone, 1 mL) were added to containers, and acetone was allowed to evaporate. Three mL of aqueous solutions of polymer at different concentrations were added to the containers which contained the pyrene residue. The aqueous solutions containing pyrene at the concentration of 6×10^{-7} M were kept at room temperature for 24 h to reach the solubilization equilibrium of pyrene in the aqueous phase. Then emission was carried at 390 nm, and excitation spectra were recorded ranging from 240 nm to 360 nm. Both excitation and emission slit widths were 10 nm. From the pyrene excitation spectra, the intensity (peak height) of 337 nm (I_{337}) was analyzed as a function of the polymer concentration. A critical micellar concentration (CMC) value was determined from the intersection of the tangent to the curve at the inflection with the horizontal tangent through the points at low concentration.

Micelle Formation

The micelles of APP-PAEMA-PCL and Gal-APP-PAEMA-PCL were prepared by a dialysis method. In brief, the corresponding polymers were dissolved in DMSO at an initial concentration of 200 mg/L, and then dialyzed against distilled water for 24 h using a dialysis tube (MWCO 8,000–12,000 g/mol).

Transmission Electron Microscopy Observation

A drop of micelle suspension was placed on a copper grid with formvar film and stained by a 0.2% (w/v) solution of phosphotungstic acid before observed by a JEM-100CX II transmission electron microscope (TEM) at an acceleration voltage of 80 keV.

Size Distribution Measurement

The zeta potential, size and size distribution of the self-assembled micelles were determined by a Zeta sizer (Nano ZS, Malvern Instruments). The solution containing micelles (200 mg/L) was passed through a 0.45 μm pore size filter prior to measurement.

Drug Loading and *In Vitro* Drug Release

The polymer (6 mg) and doxorubicin (3 mg) were dissolved in 8 mL of DMSO. The solution was placed in a dialysis tube (MWCO 8,000–12,000 g/mol) and dialyzed against 2 L of distilled water for 24 h, and the distilled water was replaced every 6 h in order to remove the unloaded free drug and DMSO. Subsequently, the dialysis tube was directly immersed into 400 mL of PBS solution (pH=7.4, I=0.2). Aliquots of 3 mL were withdrawn from the PBS periodically at 37°C. The volume of solution was held constant by adding 3 mL of PBS after each sampling. The amount of doxorubicin released from micelles was measured using UV absorbance at 497 nm. The entrapment efficiency (EE) and drug loading (DL) are defined as follows.

$$\mathrm{EE} = \frac{\text{Mass of drug loaded in micelles}}{\text{Mass of drug fed initially}} \times 100\%$$

$$\mathrm{DL} = \frac{\text{Mass of drug loaded in micelles}}{\text{Mass of drug-loaded micelles}} \times 100\%$$

Fluorescence Measurement

The fluorescence emission spectra and absorption spectra were recorded by fluorescence spectroscopy. The excitation and emission slit widths were both set at 10 nm. All the

measurements were performed within 2 h after preparation of the solutions. Stock solutions of H_2TPP (0.01 mg/mL), PAEMA-APP (0.12 mg/mL), APP-PAEMA-PCL (0.2 mg/mL), and Gal-APP-PAEMA-PCL (0.2 mg/mL) were prepared in DMSO. Each solution contains the same concentration of porphyrin (APP) moiety. The quantum yield was calculated using a secondary standard method (29). H_2TPP was used as a secondary standard. The integrated fluorescence intensities of the analyte (FA_u) and standard (FA_s), the absorbencies of the analyte (A_u) and the standard (A_s) at excitation wavelength, the excitation wavelengths of analyte (λ_u) and the standard (λ_s), and the refractive indexes of analyte solution (η_u) and standard solution (η_s) are related to the quantum yield of the analyte (ϕ_u) as follows:

$$\phi_u = \phi_s \frac{FA_u}{FA_s} \frac{A_s}{A_u} \frac{\lambda_{exs}}{\lambda_{exu}} \frac{\eta^2_u}{\eta^2_s}$$

where ϕ_s is the quantum yield of the reference standard (0.11 for H_2TPP) (30).

Dark Cytotoxicity of the Polymers

In vitro cytotoxicity was evaluated using human hepatocellular liver carcinoma (HepG2) and human laryngeal carcinoma (HEp2) cells. For dark cytotoxicity assay, 200 μL of cells in DMEM with a concentration of 2.0×10^4 cells/mL was added to each well (4.0×10^3 cells/well) in a 96-well plate. After incubation for 24 h in incubator (37°C, 5% CO_2), the culture medium in each well was replaced by 200 μL of DMEM or HEPES, respectively, containing the polymer with a particular concentration (1 mg/mL, 0.5 mg/mL, 0.25 mg/mL, 0.125 mg/mL, 0.0625 mg/mL, 0.03125 mg/mL, 0.015625 mg/mL and 0.0078125 mg/mL), and the cells were further incubated for 48 h. Then, the medium was replaced by fresh DMEM or HEPES and 20 μL of MTT solution (5 mg/mL). After incubation for 4 h, 200 μL of DMSO was added and shaken at room temperature. The optical density (OD) was measured at 570 nm with a Microplate Reader Model550 (BIO-RAD, USA). The viable rate was calculated by the following equation: cell viability=$OD_{treated}/OD_{control}$, where $OD_{control}$ was obtained in the absence of polymer and $OD_{treated}$ was obtained in the presence of polymer.

Phototoxicity of the Polymers

For phototoxicity assay, after the polymer-containing culture medium was added, the plate with cells was then placed on ice and exposed to light from a 150 W xenon lamp filtered through a 400–700 nm long-pass filter for 20 min. The cells were returned to the incubator overnight and assayed for viability. Other conditions were the same as that for dark cytotoxicity assay.

Microscopy Observation

The cells were incubated overnight before being exposed to 1 mg/mL of polymers for 24 h. For the colocalization experiments, the cells were incubated for 18 h concurrently with polymers and one of the following organelle tracers for 30 min: BODIPY FLC5-Ceramide (50 nM), LysoSensor Green (50 nM), MitoTracker Green (250 nM), and DiOC6 (5 μg/mL). Before observation, the slides were washed five times with growth medium, and then fresh medium was added. Fluorescent microscopy was performed using a confocal fluorescent microscope (C1-si, Nikon, Japan) fitted with standard FITC and Texas Red filter sets.

RESULTS AND DISCUSSION

Synthesis and Characterizations of Polymers

In this study, HEMA-PCL was synthesized by ring opening polymerization. The chemical structure of HEMA-PCL was confirmed by ^1H NMR. The peaks of terminal HEMA in HEMA-PCL appeared at 6.11 ppm and 5.58 ppm (*CH2*=*C*<), 1.91 ppm (*CH2*=*C*(*CH3*)-), and the peaks of CL units appeared at 2.14 ppm, 4.12 ppm, 1.22 ppm, 1.52 ppm, and 1.61 ppm. The signal at 3.67 ppm was assigned to the hydroxyl proton of the end group of the HEMA-PCL. The GPC analysis was employed to determine the number molecular weight of HEMA-PCL; the average number molecular weight (M_n) of HEMA-PCL was 1900 (M_w/M_n=1.23).

Synthesis of PAEMA-PCL contains two steps. First, PAEMA-CTA was prepared as a macro-RAFT agent using CTA as the chain transfer agent for RAFT polymerization. Then, PAEMA-PCL was synthesized by RAFT polymerization of HEMA-PCL with the macro-RAFT chain transfer reagent PAEMA-CTA. The molecular weights of the resultant polymer and HEMA-PCL are listed in Table I. The structure of PAEMA-PCL (in DMSO-d_6) was characterized by ^1H NMR. The signals at δ 4.05 ppm, 2.25 ppm, 1.56 ppm, 1.27 ppm in spectrum were contributed to the hydrogen proton of the PCL chains. The peaks of δ 3.89 ppm and 2.97 ppm could be assigned to the methylene hydrogen proton of PAEMA chains (Fig. S5 in Supplementary Material).

After incorporation of galactosyl moiety to PAEMA-PCL, the signals from galactosyl moiety could be detected at δ 4.05 ppm to 5.03 ppm in the ^1H NMR spectrum of Gal-PAEMA-PCL. The galactosyl substitution degree calculated from ^1H NMR is about 9%.

In the current study, porphyrin was incorporated to different polymers. The resultant polymers were characterized by fluorescence spectroscopy to determine the porphyrin substitution degree. Based on the H_2TPP standard (Fig. 1A and B), the porphyrin substitution degree is about 2% (two APP molecules per 100 AEMA units in the polymer chain) for APP-PAEMA, APP-PAEMA-PCL and Gal-APP-PAEMA-PCL.

Table I. Molecular Weights of HEMA-PCL, PAEMA, and PAEMA-PCL

Polymer	M_n	M_w/M_n
HEMA-PCL	1,900	1.23
PAEMA	16,900	1.56
PAEMA-PCL	26,300	1.58

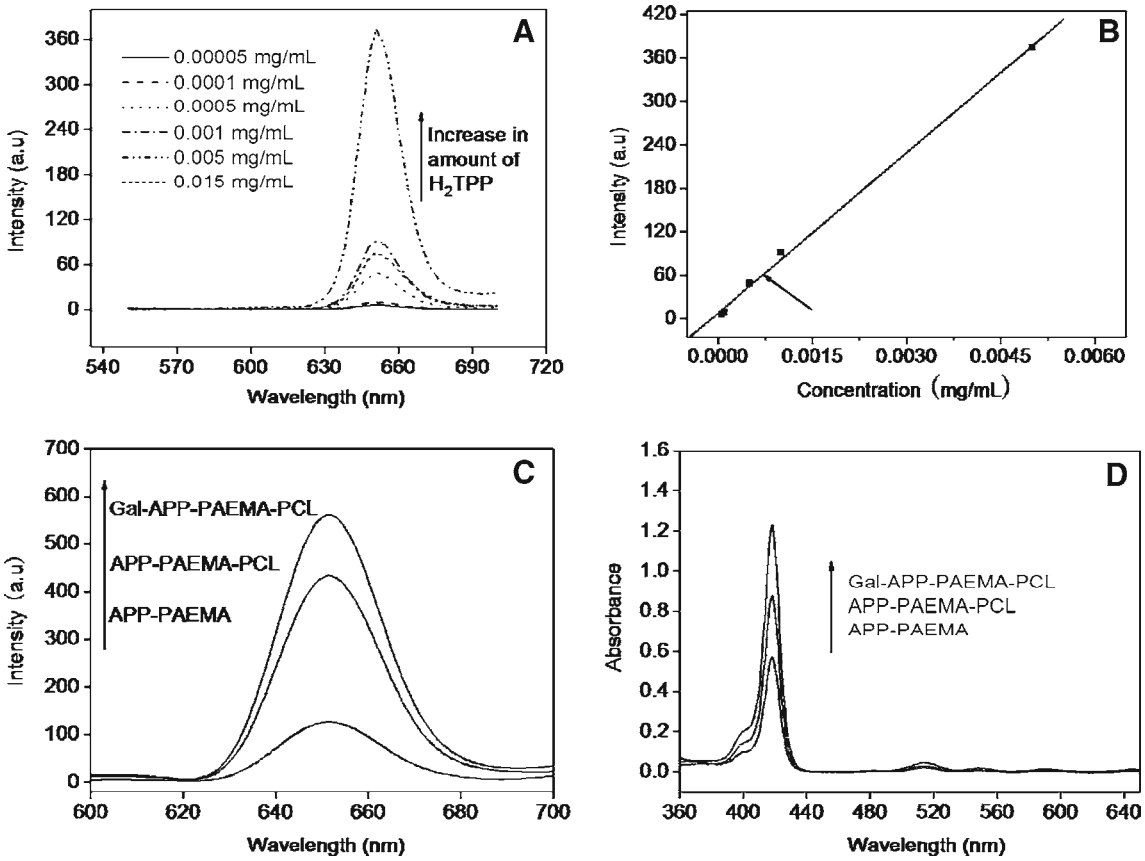

Fig. 1. The fluorescence curves of H_2TPP (**A**) and determining the amounts of APP incorporated in the polymers in DMSO (**B**). Fluorescence emission spectra (**C**) and absorption spectra (**D**) of the APP-PAEMA, APP-PAEMA-PCL and Gal-APP-PAEMA-PCL (1 mg/mL in PBS pH 7.4).

Micelle Formation and Characterizations

The structure of PAEMA-PCL and Gal-APP-PAEMA-PCL micelles was characterized by ^1H NMR (data not shown). The signals of hydrophobic PCL chains almost disappeared when the polymers were dissolved in D_2O. However, when the polymers were was dissolved in DMSO, the signals of hydrophobic PCL chains could be detected (Fig. S5 in Supplementary Material). It demonstrated the formation of the PAEMA-PCL and Gal-APP-PAEMA-PCL micelles, since the amphiphilic copolymers formed core-shell micellar structure with completely isolated hydrophobic inner cores and hydrophilic outer shells.

Furthermore, the formation of micelles was also verified by the fluorescence technique using pyrene as a probe. The fluorescence intensity increases with increasing polymer concentration, owing to the fact that pyrene has a very small absorption in aqueous solution, which increases when it is transferred into a hydrophobic environment. This effect can favor the formation of resultant micelle (31). The fluorescence intensity keeps constant at low polymer concentration, while above a certain polymer concentration, fluorescence intensity increases dramatically, indicating the formation of micelles. This polymer concentration can be defined as the critical micellar concentration (CMC). As illustrated in Fig. 2, the CMC of Gal-APP-PAEMA-PCL is 47.8 mg/L, and the CMC of APP-PAEMA-PCL is 36.9 mg/L (data not shown).

The morphology of APP-PAEMA-PCL and Gal-APP-PAEMA-PCL micelles was observed by TEM. As shown in Fig. 3, it is evident that the self-assembled micelles with a regular spherical shape are well-dispersed. From the TEM images, the sizes of micelles are less than 50 nm. Although the targeting moiety of LBA is linked to APP-PAEMA-PCL, the diameter of Gal-APP-PAEMA-PCL micelles (Fig. 3B) is almost the same as that of the APP-PAEMA-

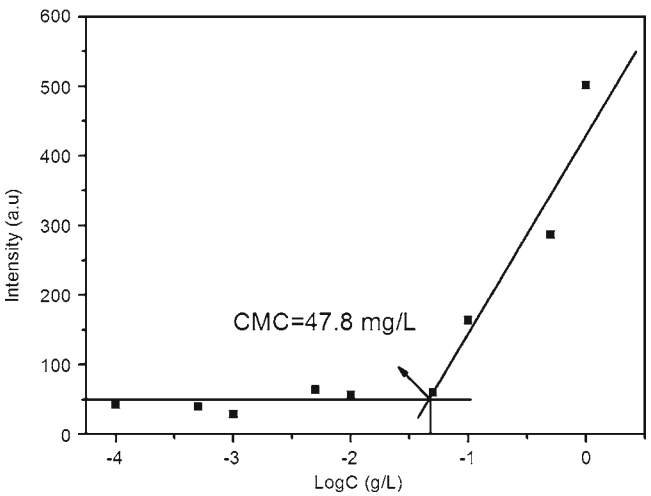

Fig. 2. The intensity of I_{337} in the excitation spectra as a function of logarithm of Gal-APP-PAEMA-PCL concentration.

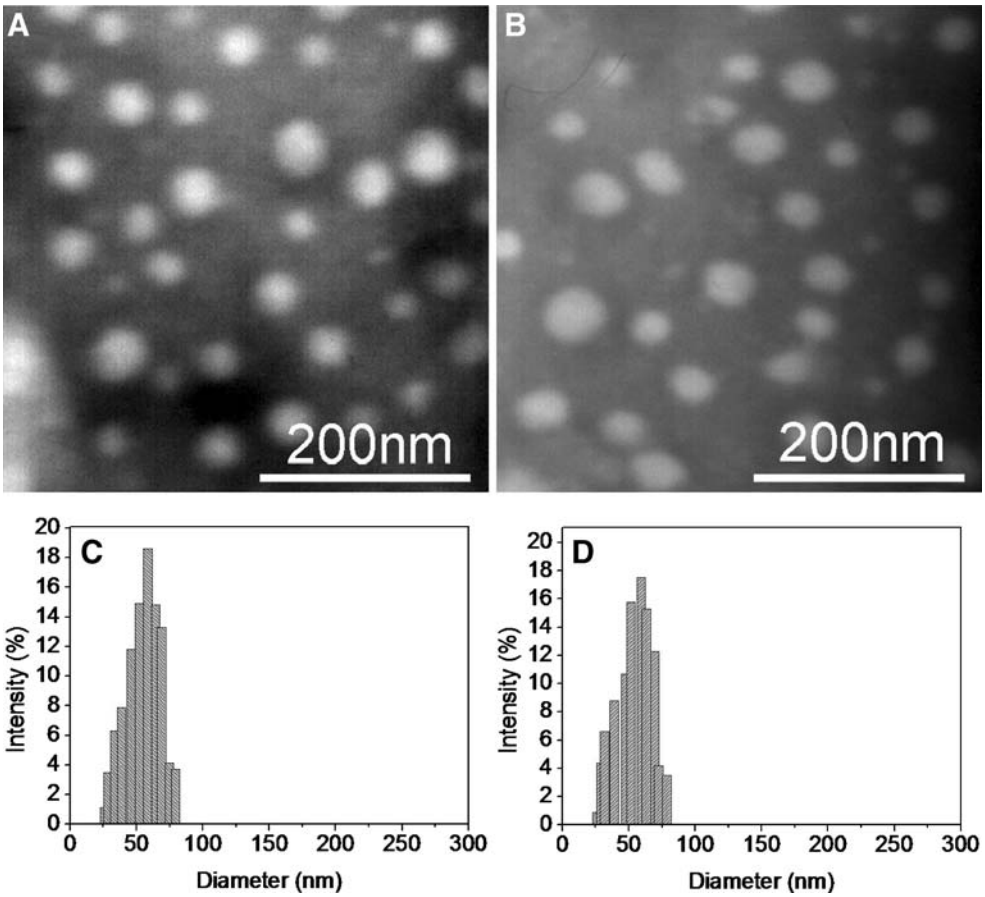

Fig. 3. TEM images of APP-PAEMA-PCL (**A**) & Gal-APP-PAEMA-PCL (**B**) micelles self-assembled in aqueous media and the size distributions of APP-PAEMA-PCL (**C**), and Gal-APP-PAEMA-PCL (**D**) determined by DLS.

PCL micelles (Fig. 3A). On the other hand, as shown in Fig. 3C and D from the dynamic light scattering (DLS), the mean sizes of APP-PAEMA-PCL micelles and Gal-APP-PAEMA-PCL micelles are 60 nm and 68 nm, respectively. The difference in the sizes determined by different methods is mainly attributed to the fact that the size measured by the DLS is the hydrodynamic diameter of micelles in aqueous solution, while the size observed by TEM is the diameter of the freeze-dried micelles. Similar difference in size on account of different measurement techniques was also found in literature (32,33).

Drug Loading and *In Vitro* Drug Release

An anticancer drug, doxorubicin, was loaded in the micelles. The EE and DL values were 15.6% and 18.2% for APP-PAEMA-PCL micelles, and 13.2% and 16.5% for Gal-APP-PAEMA-PCL micelles, respectively. The *in vitro* release profiles of doxorubicin from polymeric micelles are exhibited in Fig. 4. The release profiles of two types of micelles do not differ much. The cumulative release of Gal-APP-PAEMA-PCL micelles is slightly faster than that of APP-PAEMA-PCL micelles. The two drug release profiles shown in Fig. 4 indicated the Fickian diffusion and polymer chain relaxation were the release mechanisms for the present case. The zeta potentials of the APP-PAEMA-PCL and Gal-APP-PAEMA-PCL micelles were determined to be 8.15 mV and 6.86 mV, respectively. The positive zeta potentials were ascribed to the amino groups remaining in the polymer chains. Based on the EE (15.6% for APP-PAEMA-PCL micelles, and 13.2% for Gla-APP-PAEMA-PCL micelles) and DL (18.2% for the former and 16.5% for the latter), we can find that zeta

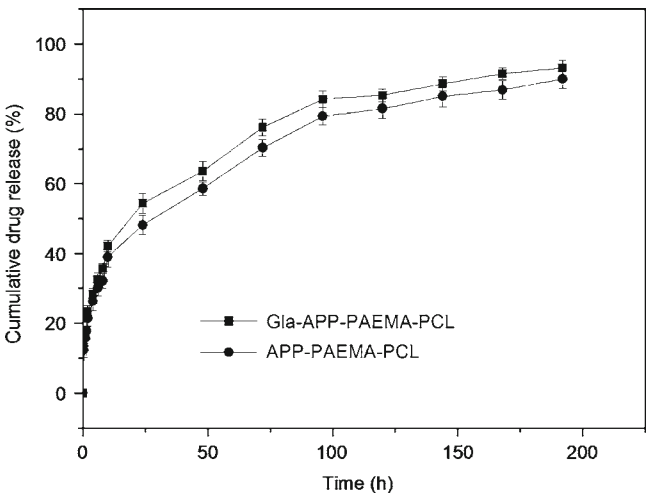

Fig. 4. Drug release from drug-loaded Gal-APP-PAEMA-PCL and APP-PAEMA-PCL micelles.

Table II. Fluorescence Quantum Yields of APP-PAEMA, APP-PAEMA-PCL, and Gal-APP-PAEMA-PCL in DMSO. (Eexcitation at 430 nm and Emission at 646 nm)

Polymer	ϕ_f
APP-PAEMA	0.1131
APP-PAEMA-PCL	0.1662
Gal-APP-PAEMA-PCL	0.1755

potential of the micelles did not affect the EE and DL of the micelles significantly. Similar result was reported elsewhere (34). At pH 7.4, amino groups in the polymer chains could not easily be protonated, and the electrostatic repulsion between the amino groups was weak. Owing to the higher zeta potential, the electrostatic repulsion between amino groups of APP-PAEMA-PCL was stronger and the micelles became a little relaxed. On the other hand, the relatively high amount of PCL segments in APP-PAEMA-PCL micelles caused the enhanced hydrophobic interaction, which resulted in more condensed hydrophobic cores and the stronger hydrophobic interaction between PCL segments and doxorubicin. As an overall result of the above two competitive factors, there was no obvious difference between the release profiles of APP-PAEMA-PCL micelles and Gla-APP-PAEMA-PCL micelles.

Fluorescence Measurement

As we know, conventional photosensitizers easily form aggregates as a result of their π-π interactions and hydrophobic characteristics, leading to self-quenching effect of the excited state. For photodynamic therapy, low tendency to aggregation in an aqueous media is the important requirement for the photodynamic agents. Thus, in our study, we measured the fluorescence quantum yields of APP-PAEMA, APP-PAEMA-PCL, and Gal-APP-PAEMA-PCL (Table II). The polymers showed high fluorescence quantum yields, which indicated that these polymers had the low tendency to aggregation.

It was found that fluorescence quantum yields increased in the order of APP-PAEMA<APP-PAEMA-PCL<Gal-APP-PAEMA-PCL. It was ascribed to the presence of PAEMA and PAEMA-PCL segments conjugated to the APP, which could prevent the porphyrin macrocylces from overlapping each other. Thus the fluorescence quantum yields increased. The similar findings were also reported elsewhere (35).

As demonstrated in Fig. 1C and D, the intensities of fluorescence emission and absorption of Gla-APP-PAEMA-PCL and APP-PAEMA-PCL are higher than that of PAEMA-APP. The reason might be the formation

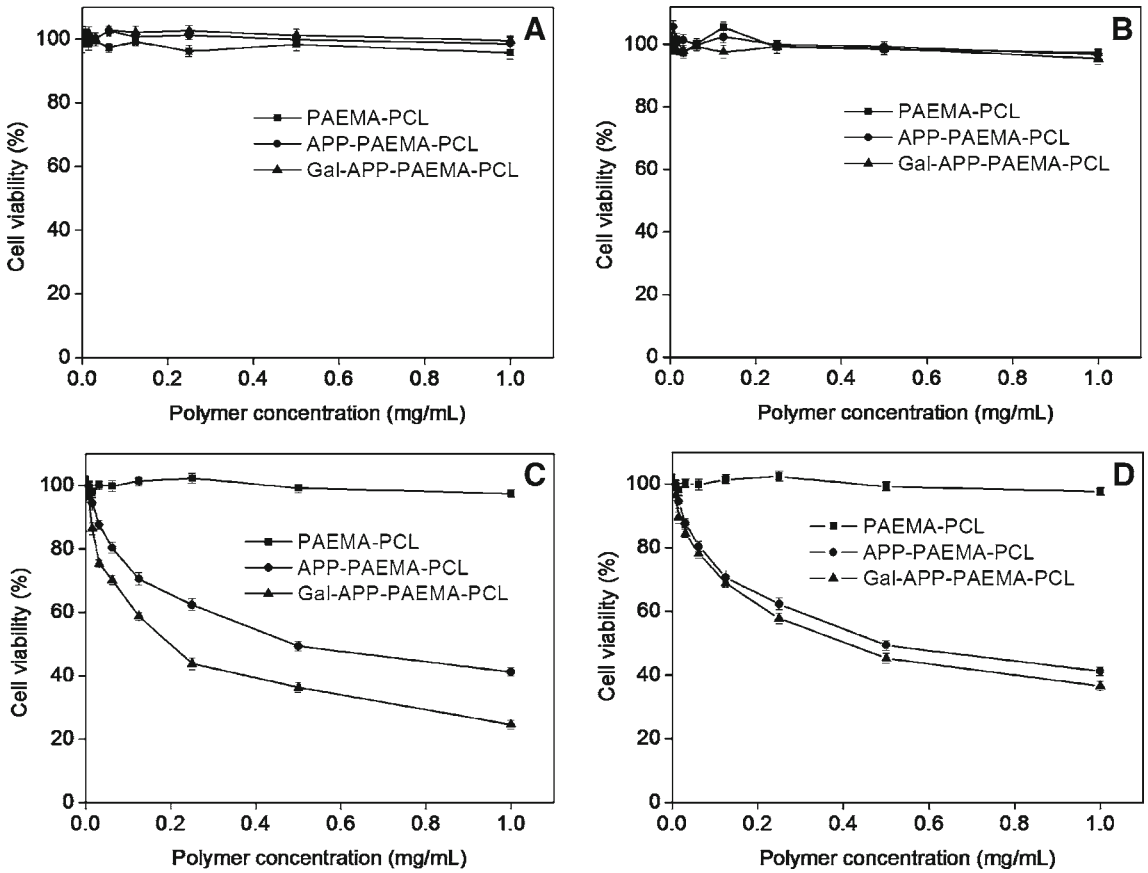

Fig. 5. Dark toxicity of polymers for (**A**) HepG2 cells and (**B**) HEp2 cells, and phototoxicity of polymers for (**C**) HepG2 cells and (**D**) HEp2 cells.

of micelles for APP-PAEMA-PCL and Gla-APP-PAEMA-PCL, which could prevent the fluorescence quenching. With the hydrophilic galactosyl moiety incorporated to the polymer, the Gla-APP-PAEMA-PCL micelles were more stable in the aqueous medium, thus the fluorescence intensity of Gla-APP-PAEMA-PCL was higher than that of APP-PAEMA-PCL.

Dark Toxicity and Phototoxicity of Polymers

As shown in Fig. 5, no significant decrease in cell viability when the concentration of the polymer is below 1 mg/mL could be observed for HepG2 (Fig. 5A) and HEp2 (Fig. 5B) cells. Obviously, all polymers have no apparent dark cytotoxicity.

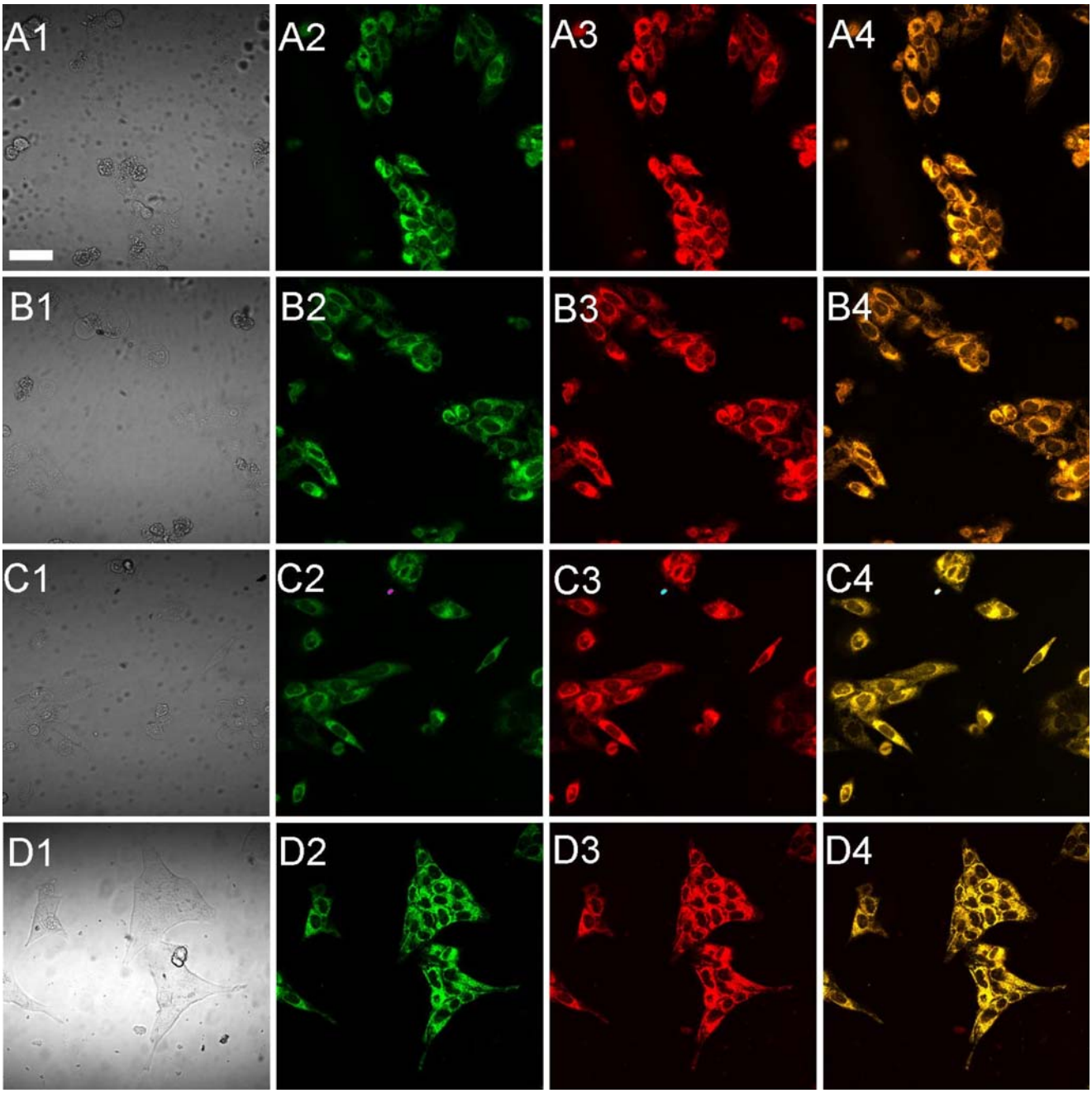

Fig. 6. Images of HepG2 cells co-incubated with Gal-APP-PAEMA-PCL micelles. (**A1, B1, C1, D1**) Phase contrast images, (**A2**) fluorescence image of BODIPY ceramide-labeled cells, (**B2**) fluorescence image of LysoSensor green-labeled cells, (**C2**) fluorescence image of MitoTracker green-labeled cells, (**D2**) fluorescence image of DiOC6-labeled cells, (**A3, B3, C3, D3**) fluorescence images of the cells with fluorescence from porphyrin moieties in Gal-APP-PAEMA-PCL micelles. (**A4, B4, C4, D4**) fluorescence images of the cells with overlapped fluorescence from the organelle tracer and fluorescence from porphyrin moieties. Scale bar: 50 μm.

In contrast, all porphyrin-incorporated polymers show phototoxicity toward HEp2 cells and HepG2 cells. IC_{50} values of Gal-APP-PAEMA-PCL and APP-PAEMA-PCL for HepG2 cells are 0.2 mg/mL and 0.5 mg/mL, respectively (Fig. 5C), while IC_{50} values of Gal-APP-PAEMA-PCL and APP-PAEMA-PCL for HEp2 cells are 0.4 mg/mL and 0.5 mg/mL, respectively (Fig. 5D). Gal-APP-PAEMA-PCL, bearing hepatic targeting moieties, exhibits the highest phototoxicity for HepG2 cells. It was reported that asialoglycoprotein (ASGP) receptors were expressed plentifully on the surface of hepatoma cells (20,21), and targeting could be accomplished through introduction of galactose residues, such as terminal β-D-galactose and N-acetylgalactosamine residues, which could bind specifically to the ASGP receptors. In our study, the internalization of Gal-APP-PAEMA-PCL for HepG2 cells is higher compared with the polymers without targeting groups. For receptor-negative HEp2 cells, Gal-APP-PAEMA-PCL also exhibits slightly higher phototoxicity than

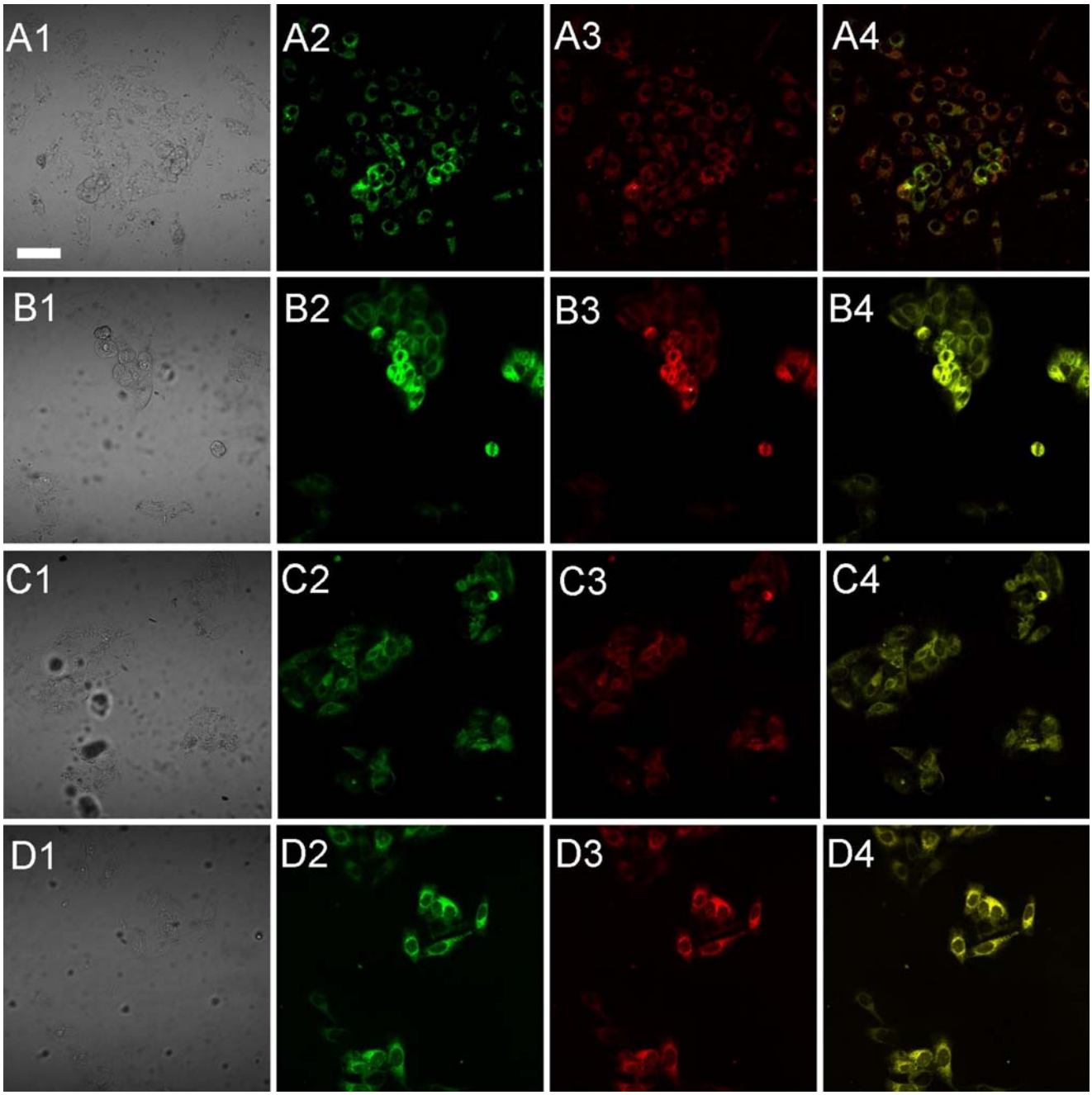

Fig. 7. Images of HepG2 cells co-incubated with APP-PAEMA-PCL micelles. (**A1, B1, C1, D1**) Phase contrast images, (**A2**) fluorescence image of BODIPY ceramide-labeled cells, (**B2**) fluorescence image of LysoSensor green-labeled cells, (**C2**) fluorescence image of MitoTracker green-labeled cells, (**D2**) fluorescence image of DiOC6-labeled cells, (**A3, B3, C3, D3**) fluorescence images of the cells with fluorescence from porphyrin moieties in APP-PAEMA-PCL micelles. (**A4, B4, C4, D4**) fluorescence images of the cells with overlapped fluorescence from the organelle tracer and fluorescence from porphyrin moieties. Scale bar: 50 μm.

that of APP-PAEMA-PCL (Fig. 5D). This may be attributed to the higher hydrophilicity of Gal-APP-PAEMA-PCL.

Cell Internalization of APP-PAEMA-PCL and Gal-APP-PAEMA-PCL

The subcellular localization of APP-PAEMA-PCL and Gal-APP-PAEMA-PCL in HepG2 cells and HEp2 cells after 24 h co-incubation with the polymer were investigated using fluorescence microscopy. As shown in Figs. 6, 7, 8 and 9, the preferential sites of intracellular localization were found to be the lysosomes of HepG2 and HEp2 cells for both APP-PAEMA-PCL and Gal-APP-PAEMA-PCL. These results imply that pH-responsive behavior of the micelles due to the existence of amino groups in PAEMA segments played an important role in determining the preferential localization sites of the polymers within cells. As we know, due to the pH-responsive behavior of the polymers, the micelles accumulate

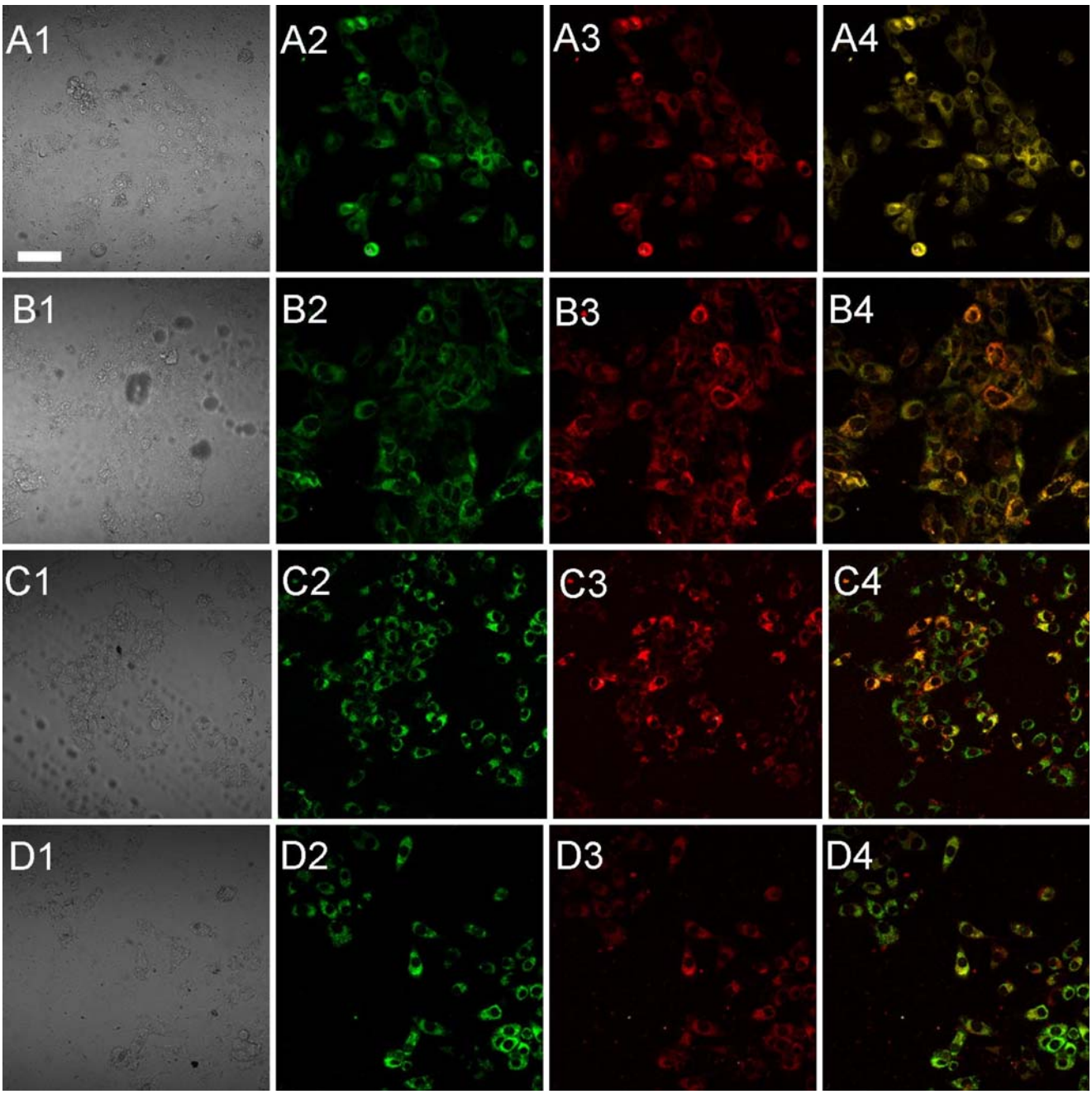

Fig. 8. Images of HEp2 cells co-incubated with Gal-APP-PAEMA-PCL micelles. (**A1, B1, C1, D1**) Phase contrast images, (**A2**) fluorescence image of BODIPY ceramide-labeled cells, (**B2**) fluorescence image of LysoSensor green-labeled cells, (**C2**) fluorescence image of MitoTracker green-labeled cells, (**D2**) fluorescence image of DiOC6-labeled cells, (**A3, B3, C3, D3**) fluorescence images of the cells with fluorescence from porphyrin moieties in Gal-APP-PAEMA-PCL micelles. (**A4, B4, C4, D4**) fluorescence images of the cells with overlapped fluorescence from the organelle tracer and fluorescence from porphyrin moieties. Scale bar: 50 μm.

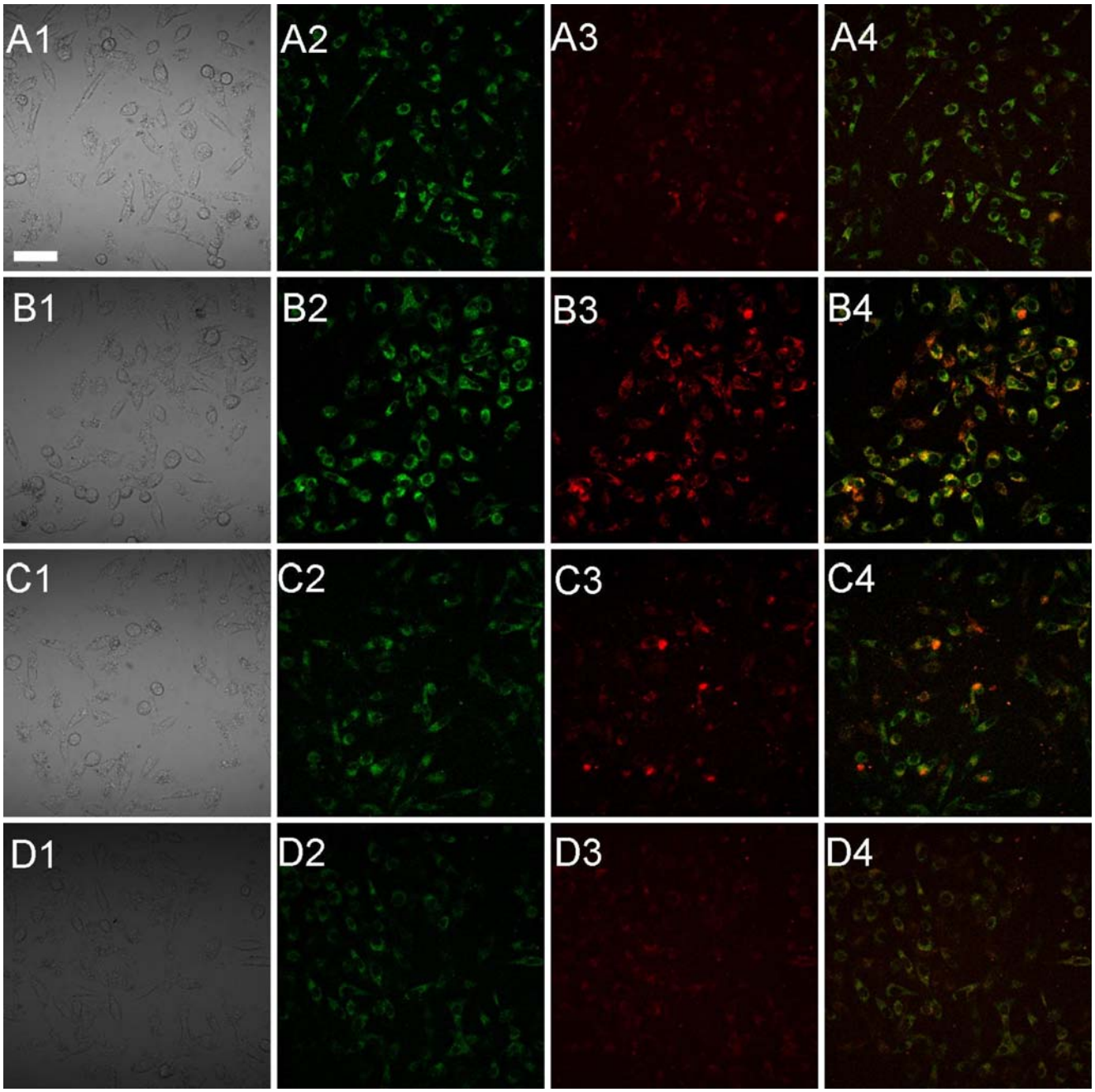

Fig. 9. Images of HEp2 cells co-incubated with APP-PAEMA-PCL micelles. (**A1, B1, C1, D1**) Phase contrast images, (**A2**) fluorescence image of BODIPY ceramide-labeled cells, (**B2**) fluorescence image of LysoSensor green-labeled cells, (**C2**) fluorescence image of MitoTracker green-labeled cells, (**D2**) fluorescence image of DiOC6-labeled cells, (**A3, B3, C3, D3**) fluorescence images of the cells with fluorescence from porphyrin moieties in APP-PAEMA-PCL micelles. (**A4, B4, C4, D4**) fluorescence images of the cells with overlapped fluorescence from the organelle tracer and fluorescence from porphyrin moieties. Scale bar: 50 μm.

effectively in solid tumors because of the low pH value of the tumor tissues and in the endosomal compartments in the tumor cells (36,37).

The amount of Gal-APP-PAEMA-PCL in HepG2 cells was higher as compared with Gal-APP-PAEMA-PCL in HEp2 cells, and APP-PAEMA-PCL within HepG2 and HEp2 cells. The reason was that ASGP receptors were expressed plentifully on the surface of HepG2 cells, and Gal-APP-PAEMA-PCL had the target ligands (21).

CONCLUSIONS

In summary, Gal-APP-PAEMA-PCL and APP-PAEMA-PCL polymers were synthesized by ring opening polymerization and RAFT polymerization. The resulting polymers are able to self-assemble to form stable micelles. Compared to the APP-PAEMA, the fluorescence intensity of the APP-PAEMA-PCL and Gal-APP-PAEMA-PCL are higher. None of the porphyrin-incorporated polymers exhibit dark cytotox-

icity to both HEp2 cells and HepG2 cells. Importantly, Gal-APP-PAEMA-PCL micelles could be selectively recognized by HepG2 cells and subsequently preferentially accumulate in HepG2 cells, resulting in the higher phototoxicity effect.

ACKNOWLEDGEMENT

The financial supports from National Natural Science Foundation of China (50633020), Ministry of Science and Technology of China (2005CB623903) and Ministry of Education of China (Cultivation Fund of Key Scientific and Technical Innovation, Project 707043) are gratefully acknowledged.

REFERENCES

1. Detty MR, Gibson SL, Wanger SJ. Current clinical and preclinical photosensitizers for use in photodynamic therapy. J Med Chem. 2004;47:3897–915.
2. Kessel D. Relocalization of cationic porphyrins during photodynamic therapy. Photochem Photobiol Sci. 2002;11:837–40.
3. Banfi S, Caruso E, Caprioli S, Mazzagatti L, Canti G, Ravizza R, *et al*. Photodynamic effects of porphyrin and chlorin photosensitizers in human colon adenocarcinoma cells. Bioorg Med Chem. 2004;12:4853–60.
4. Castano AP, Liu Q, Hamblin MR. A green fluorescent protein-expressing murine tumour but not its wild-type counterpart is cured by photodynamic therapy. Br J Cancer. 2006;13:391–7.
5. Nishiyama N, Stapert HR, Zhang GD, Takasu D, Jiang DL, Nagano T, *et al*. Light-harvesting ionic dendrimer porphyrins as new photosensitizers for photodynamic therapy. Bioconjugate Chem. 2003;14:58–66.
6. Sharman WM, Allen CM, van Lier JE. Photodynamic therapeutics: basic principles and clinical applications. Drug Discov Today. 1999;11:507–17.
7. Desjardins A, Flemming J, Sternberg ED, Dolphin D. Nitrogen extrusion from pyrazoline-substituted porphyrins and chlorins using long wavelength visible light. Chem Commun. 2002;22:2622–3.
8. Li H, Fedorova OS, Trumble WR, Fletcher TR, Czuchajowski L. Site-specific photomodification of DNA by porphyrinoligonucleotide conjugates synthesized via a solid-phase H-phosphonate approach. Bioconjugate Chem. 1997;8:49–56.
9. Hamblin MR, Newman EL. Photosensitizer targeting in photodynamic therapy. II. Conjugates of haematoporphyrin with serum lipoproteins. J Photochem Photobiol B: Bio. 1994;26:147–57.
10. Gijsens A, Missiaen L, Merlevede W, de Witte P. Epidermal growth factor-mediated targeting of chlorin e_6 selectively potentiates its photodynamic activity. Cancer Res. 2000;60:2197–202.
11. Hudson R, Carcenac M, Smith K, Madden L, Clarke OJ, Pelegrin A, *et al*. The development and characterization of porphyrin isothiocyanate-monoclonal antibody conjugates for photoimmunotherapy. Br J Cancer. 2005;92:1442–9.
12. Li G, Pandey SK, Graham A, Dobhal MP, Mehta R, Chen Y, *et al*. Functionalization of OEP-based benzochlorins to develop carbohydrateconjugated photosensitizers. Attempt to target beta-galactosiderecognized proteins. J Org Chem. 2004;69:158–72.
13. Chen X, Gentry C, Kopeckova P, Kopecek J. HPMA copolymer-anticancer drug-OV-TL16 antibody conjugates. II. Processing in epithelial ovarian carcinoma cells *in vitro*. Int J Cancer. 1998; 75:600–8.
14. Soukos NS, Hamblin MR, Hasan T. The effect of charge on cellular uptake and phototoxicity of polylysine chlorin(e_6) conjugates. Photochem Photobiol. 1997;65:723–9.
15. Pandey RK, Smith NW, Shiau FY, Dougherty TJ, Smith KM. Syntheses of cationic porphyrins and chlorines. J Chem Soc Chem Commun. 1991;22:1637–8.
16. Oseroff AR, Ohuoha D, Ara G, McAuliffe D, Foley J, Cincotta L. Intramitochondrial dyes allow selective *in vitro* photolysis of carcinoma cells. Proc Natl Acad Sci USA. 1986;83:9729–33.
17. Park EK, Lee SB, Lee YM. Preparation and characterization of methoxy poly(ethylene glycol)/poly(epsilon-caprolactone) amphiphilic block copolymeric nanospheres for tumor-specific folate-mediated targeting of anticancer drugs. Biomaterials. 2005;26:1053–61.
18. Bae Y, Fukushima S, Harada A, Kataoka K. Design of environment-sensitive supramolecular assemblies for intracellular drug delivery: polymeric micelles that are responsive to intracellular pH change. Angew Chem Int Ed. 2003;42:4640–3.
19. Nasongkla N, Shuai X, Ai H, Weinberg BD, Pink J, Boothman DA. cRGD-functionalized polymer micelles for targeted doxorubicin delivery. Angew Chem Int Ed. 2004;43:6323–7.
20. Fallon RJ, Schwartz AL. Receptor-mediated delivery of drugs to hepatocytes. Adv Drug Deliv Rev. 1989;4:49–63.
21. Donati I, Gamini A, Vetere A, Campa C, Paoletti S. Synthesis, characterization, and preliminary biological study of glycoconjugates of poly(styrene-co-maleic acid). Biomacromolecules. 2002;3:805–12.
22. Eisenberg C, Seta N, Appel M, Feldmann G, Durand G, Feger J. Asialoglycoprotein receptor in human isolated hepatocytes from normal liver and its apparent increase in liver with histological alterations. J Hepatol. 1991;13:305–9.
23. Ashwell G, Harford J. Carbohydrate-specific receptors of the liver. Annu Rev Biochem. 1982;51:531–54.
24. Adler AD, Longo FR, Shergalis W. Mechanistic investigations of porphyrin syntheses. I. preliminary studies on ms-tetraphenylporphin. J Am Chem Soc. 1964;86:3145–9.
25. Kruper WJ, Chamberlin TA, Kochanny M. Regiospecific aryl nitration of meso-substituted tetraarylporphyrins: a simple route to bifunctional porphyrins. J Org Chem. 1989;54:2753–6.
26. Wu DQ, Sun YX, Xu XD, Cheng SX, Zhang XZ, Zhuo RX. Biodegradable and pH-sensitive hydrogels for cell encapsulation and controlled drug release. Biomacromolecules. 2008;9:1155–62.
27. Wei H, Zhang XZ, Zhou Y, Cheng SX, Zhuo RX. Self-assembled thermoresponsive micelles of poly(N-isopropylacrylamide-b-methyl methacrylate). Biomaterials. 2006;27: 2028–34.
28. Zhu JL, Zhang XZ, Cheng H, Li YY, Cheng SX, Zhuo RX. Synthesis and characterization of well-defined, amphiphilic Poly (N-isopropylacrylamide)-b-[2-hydroxyethyl methacrylate- poly(ε-caprolactone)]$_n$ graft Copolymers by RAFT polymerization and macromonomer method. J Polym Sci Pol Chem. 2007;45:5354–64.
29. Velapoldi RA, Tønnesen HH. Corrected emission spectra and quantum yields for a series of fluorescent compounds in the visible spectral region. J Fluoresc. 2004;14:465–72.
30. Seybold PG, Gouterman M. Porphyrins: XIII: fluorescence spectra and quantum yields. J Mol Spectrosc. 1969;31:1–13.
31. Inoue T, Chen G, Nakamae K, Hoffman AS. An AB block copolymer of oligo(methyl methacrylate) and poly(acrylic acid) for micellar delivery of hydrophobic drugs. J Control Release. 1998;51:221–9.
32. Morita T, Horikiri Y, Suzuki T, Yoshino H. Preparation of gelatin microparticles by co-lyophilization with poly(ethylene glycol): characterization and application to entrapment into biodegradable microspheres. Int J Pharm. 2001;219:127–37.
33. Giacomelli C, Schmidt V, Borsali R. Nanocontainers formed by self-assembly of poly(ethylene oxide)-*b*-poly(glycerol monomethacrylate)-drug conjugates. Macromolecules. 2007; 40:2148–57.
34. Ye YQ, Yang FL, Hu FQ, Du YZ, Yuan H, Yu HY. Core-modified chitosan-based polymeric micelles for controlled release of doxorubicin. Int J Pharm. 2008;352:294–301.
35. Kanofsky JR. Quenching of singlet oxygen by human plasma. Photochem Photobiol. 1990;51:299–303.
36. Kornguth SE, Kalinke T, Robins HI, Cohen JD, Turski P. Preferential binding of radiolabeled Poly-L-lysines to C6 and U87 MG glioblastomas compared with endothelial cells *in vitro*. Cancer Res. 1989;49:6390–5.
37. Sibrian-Vazquez M, Jensen TJ, Fronczek FR, Hammer RP, Vicente MGH. Synthesis and characterization of positively charged porphyrin-peptide conjugates. Bioconjugate Chem. 2005;16:852–63.